



# **Mars Science Laboratory**

## **Pointing, Positioning, Phasing, and Coordinate Systems (PPPCS) Document, Volume 9**

### **Surface Remote Sensing and Navigation**

**Rev. Public Release**

**13 May 2016**

Steve Peters  
Surface Attitude, Positioning, and Pointing Lead

This research was carried out at the Jet Propulsion Laboratory, California Institute of Technology, under a contract with the National Aeronautics and Space Administration.



Jet Propulsion Laboratory  
California Institute of Technology  
Pasadena, California

## Table of Contents

<b>1.0</b>	<b>About This Document</b>	<b>1</b>
1.1	Scope	1
1.2	Acknowledgements	1
<b>2.0</b>	<b>Surface Sensors and Actuators</b>	<b>2</b>
2.1	Sensors	2
2.1.1	Rover Engineering Cameras	2
2.1.1.1	Engineering Camera Images	2
2.1.1.2	Navcam Description	3
2.1.1.3	Navcam Clocking	4
2.1.1.4	Navcam Pointing	5
2.1.1.5	Hazcam Description	5
2.1.1.6	Hazcam Clocking	6
2.1.1.7	Hazcam Pointing	8
2.1.2	ChemCam and Mastcam Pointing	10
2.1.3	MARDI Pointing	10
2.1.4	RAD and REMS Pointing	10
2.1.5	Chassis-mounted Fiducial Locations	11
2.2	Actuators	14
2.2.1	Remote Sensing Mast (RSM)	14
2.2.1.1	The RSM Elevation Actuator	14
2.2.1.2	The RSM Azimuth Actuator	14
2.2.1.3	RSM Forward Kinematics and Pointing	15
2.2.1.4	Calibration Targets for RSM Instruments	19
2.2.2	Mobility	22
2.2.2.1	Steering Actuators	22
2.2.2.2	Drive Actuators	23
2.2.2.3	Passive Suspension Sensors	23
2.2.2.4	Mobility Forward Kinematics	25
2.2.2.5	Mobility-mounted Fiducials	29

## Figure Index

---

Figure 1. Notational conventions.....	2
Figure 2. Blooming, image transfer smear, dark current, and $\frac{1}{4}$ resolution pixels relative to the CCD frame transfer direction.....	3
Figure 3. Navcam locations at the top of the RSM.....	3
Figure 4. Front view of the rover with RSM instruments pointing in the rover mechanical frame +X direction (the rover mechanical frame X vector is out of the page).....	4
Figure 5. Navcam frame transfer direction.....	4
Figure 6. Navcam frame transfer directions as mounted on the RSM.....	5
Figure 7. Clocking effects on the appearance of Navcam images.....	5
Figure 8. Locations of the Hazcams -- side view.....	6
Figure 9. Hazcam frame transfer direction.....	6
Figure 10. Front Hazcam locations and frame transfer directions as mounted.....	7
Figure 11. Rear Hazcam locations and frame transfer directions as mounted.....	7
Figure 12. Clocking effects on the appearance of Hazcam images.....	8
Figure 13. Deck and wheel restraint fiducials.....	12
Figure 14. OCM fiducials.....	12
Figure 15. RSM elevation actuator joint angles.....	14
Figure 16. RSM azimuth actuator joint angles.....	15
Figure 17. RSM azimuth and elevation coordinate frames relative to the rover mechanical frame and the ChemCam boresight when pointing straight forward.....	16
Figure 18. The frame tree for RSM pointing.....	18
Figure 19. The ChemCam calibration target.....	19
Figure 20. The Mastcam calibration target.....	19
Figure 21. Steering direction.....	23
Figure 22. Drive direction.....	23
Figure 23. The mobility suspension system.....	24
Figure 24. Suspension sensor $0^\circ$ references and + and - range of motion (the rover mechanical frame Y vector is into the page).....	24
Figure 25. Mobility frame tree.....	25
Figure 26. Mobility suspension and steering frame orientations.....	26
Figure 27. Fiducials mounted on the mobility system.....	29
Figure 28. Mobility fiducial frame tree.....	30

## Table Index

---

Table 1. Hazcam names .....	8
Table 2. Translational and angular offsets relating Hazcam boresight vectors to the rover mechanical frame .....	8
Table 3. Translational and angular offsets relating the MARDI boresight to the rover mechanical frame.....	10
Table 4. Translational and angular offsets relating RAD and REMS sensor orientation to the rover mechanical frame.....	11
Table 5. Translational offsets relating chassis-mounted fiducials to the rover mechanical frame .....	13
Table 6. RSM pointing frame and vector names .....	15
Table 7. Rotation matrices relating RSM azimuth and elevation actuator frames to their parent frames .....	16
Table 8. Translational offsets relating RSM azimuth and elevation actuator frames to their parent frames.....	17
Table 9. Translational and angular offsets relating RSM boresight vectors to the RSM elevation frame .....	17
Table 10. The boresight unit vector in the RSM elevation frame.....	19
Table 11. RSM calibration target names.....	20
Table 12. Translational and angular offsets relating RSM calibration target normal vectors to the rover mechanical frame.....	20
Table 13. Mobility frame names.....	25
Table 14. Rotation matrices relating mobility frames to their parent frames .....	26
Table 15. Translational offsets relating mobility frames to their parent frames.....	27
Table 16. Mobility fiducial names .....	29
Table 17. Translational offsets relating the centers of mobility fiducials to their parent frames .....	30

## **1.0 About This Document**

### **1.1 Scope**

This document defines coordinate system, pointing, polarity, and phasing information for the Remote Sensing Mast (RSM) and chassis-mounted science payload instruments, and for the Mobility system. This document also defines and documents coordinate system, phasing, and range-of-motion information for RSM and mobility system actuators and passive articulations. Finally, it includes the locations and orientations of chassis-mounted calibration targets for RSM-mounted instruments, and chassis-mounted and mobility-mounted fiducials.

### **1.2 Acknowledgements**

Figures and values representing the mechanical design were provided by Chris Voorhees, Peter Illsley, Dave Johnson, Jaime Waydo, Milo Silverman, Bill Allen, Paul Lytal, and many others. Engineering camera information was provided by Justin Maki.

## 2.0 Surface Sensors and Actuators

The phasing described in this document is the high level seen by the user and some high-level software.

Notational conventions adopted in the sections that follow are listed in Figure 1.

	axis out of the page
	axis into the page
<b>X</b>	coordinate frame axis label (without sign)
<b>+X</b>	axis direction label (with sign)
<b>[+91°]</b>	value as designed -- actual to be determined in ATLO
<b>(+45°)</b>	value as designed -- not directly measured in ATLO
$\theta_{\text{joint}}$	$\theta$ used for all joint angles, subscript indicates joint
$\varphi_{\text{axis}}$	$\varphi$ used for all rotations about an axis of a coordinate system, subscript indicates axis

**Figure 1. Notational conventions**

### 2.1 Sensors

This section describes phasing and pointing information for the engineering cameras. It also includes pointing information for RSM-mounted and chassis-mounted science instruments. Locations and orientations of calibration targets for RSM-mounted science instruments, and locations of chassis-mounted fiducials, are also described.

#### 2.1.1 Rover Engineering Cameras

##### 2.1.1.1 Engineering Camera Images

The CCDs for MSL's Navcams and Hazcams have the same imaging characteristics. The description here applies to both Navcams and Hazcams.

Exposures are not shuttered, but achieved by first removing accumulated charge from all of the pixels in the array, pausing for the desired exposure time, and then shifting the charges row by row to neighboring rows until they reach the edge row from which they are digitized and transferred as serial data to the camera interface board. During the transfer process, each pixel receives charge both from its neighbor pixel in its neighboring row and from light from the scene, resulting in frame transfer smear. When the accumulated charge from the exposure is significantly larger than the added charge due to exposure during frame transfer, frame transfer smear can be insignificant; but when a bright feature is present in the image (such as the sun or sun glint off of a specular surface), the smear can be clearly visible.

Blooming (overflow of charge from a pixel to its neighbors, resulting in white streaks in the image) occurs preferentially in the column direction, aligned with frame transfer smear.

Brightening of the image due to dark current is significantly increased at high CCD temperatures. Dark current accumulates during exposure and frame transfer. Portions of the images transferred longer distances accumulate more dark current than portions transferred shorter distances and can appear brighter.

The clocking of camera installation affects the resulting directions of frame transfer smear and blooming, and which side is brighter when affected by dark current. Figure 2 shows the relationships between these directions. The direction of pixel binning for  $\frac{1}{4}$  resolution images is also shown.

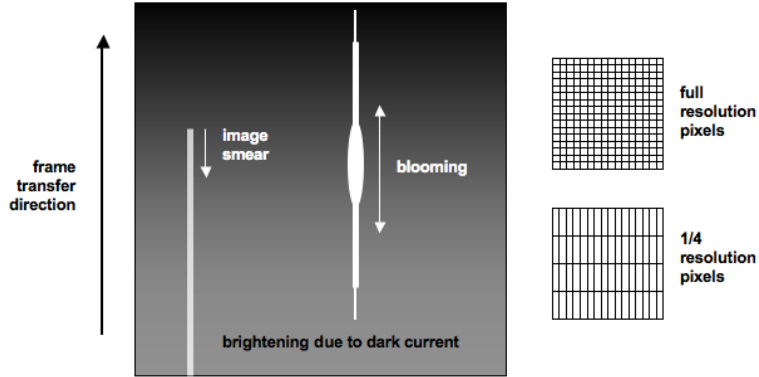


**Figure 2. Blooming, image transfer smear, dark current, and 1/4 resolution pixels relative to the CCD frame transfer direction**

### 2.1.1.2 Navcam Description

MSL has four Navcams mounted on its Remote Sensing Mast (RSM): left and right Navcams A form the primary stereo pair, connected to Rover Compute Element A (RCE-A); and the left and right Navcams B form a backup stereo pair, connected to Rover Compute Element B (RCE-B). The designations left and right are with respect to the viewing direction.

Each Navcam has a 45° field-of-view (FOV) f-tan(theta) lens and a 1024x1024 pixel detector array.

Navcam images are used by operators on the ground to view the terrain around the rover, and are used both in onboard and ground-based stereo image processing to derive range maps of the surface. These range data are used for mobility hazard detection, for designation of targets, and for determination of the location of the surface in the sample acquisition workspace in support of surface contact operations.

The locations of the four Navcams are shown in Figure 3. Science instruments are also shown.

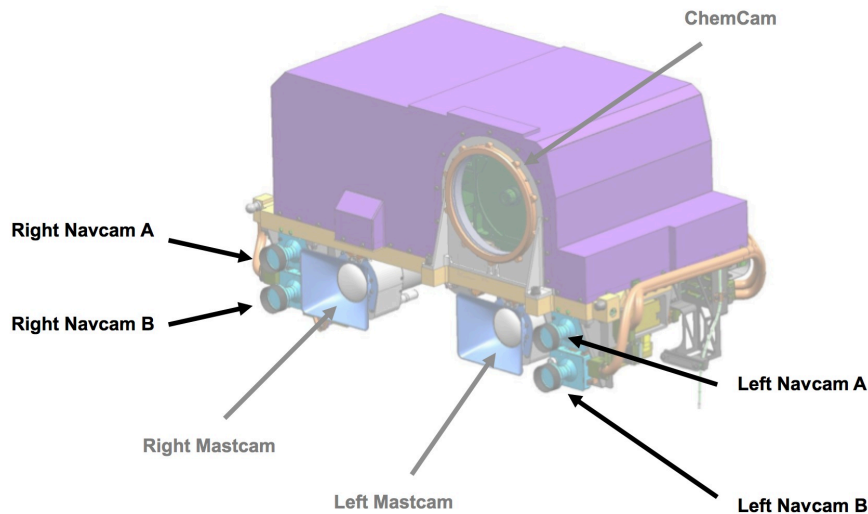


**Figure 3. Navcam locations at the top of the RSM**

A view of the front of the rover with RSM azimuth and elevation actuators pointing the four Navcam and the ChemCam uncalibrated (see discussion below) boresights in the direction of the +X axis of the rover mechanical frame is shown in Figure 4. (The Mastcams are "toed in" with respect to this direction.) RSM azimuth and elevation joint angles are defined in sections 0 and 2.2.1.1 below.

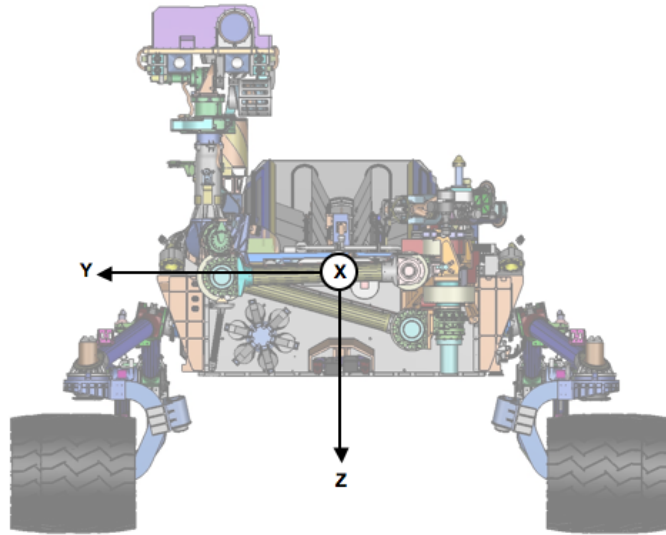


**Figure 4. Front view of the rover with RSM instruments pointing in the rover mechanical frame +X direction (the rover mechanical frame X vector is out of the page)**

### 2.1.1.3 Navcam Clocking

Each precise Navcam "boresight" alignment is determined by camera calibration procedures performed in ATLO, and is embodied in a camera model which provides mapping between the vectors from each of the pixels of the camera out into the world with reference to a fixed rover frame, measured with respect to datum targets and/or secondary fiducials.

Navcam frame transfer directions are shown in Figure 5 and Figure 6. Frame transfer direction is shown relative to the camera CCD.

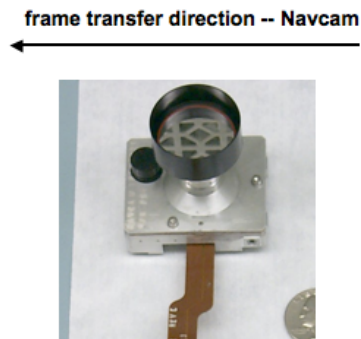


**Figure 5. Navcam frame transfer direction**

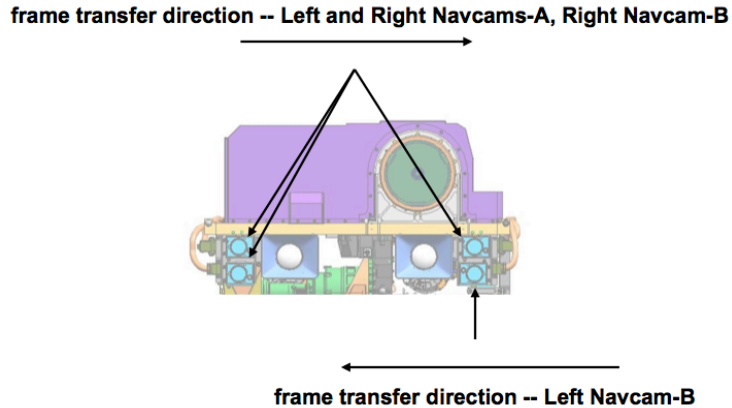


**Figure 6. Navcam frame transfer directions as mounted on the RSM**

The effects of clocking on the appearance of Navcam images are shown in Figure 7. Dotted yellow boxes indicate the third of the image which is usable for sun sensing for attitude determination.

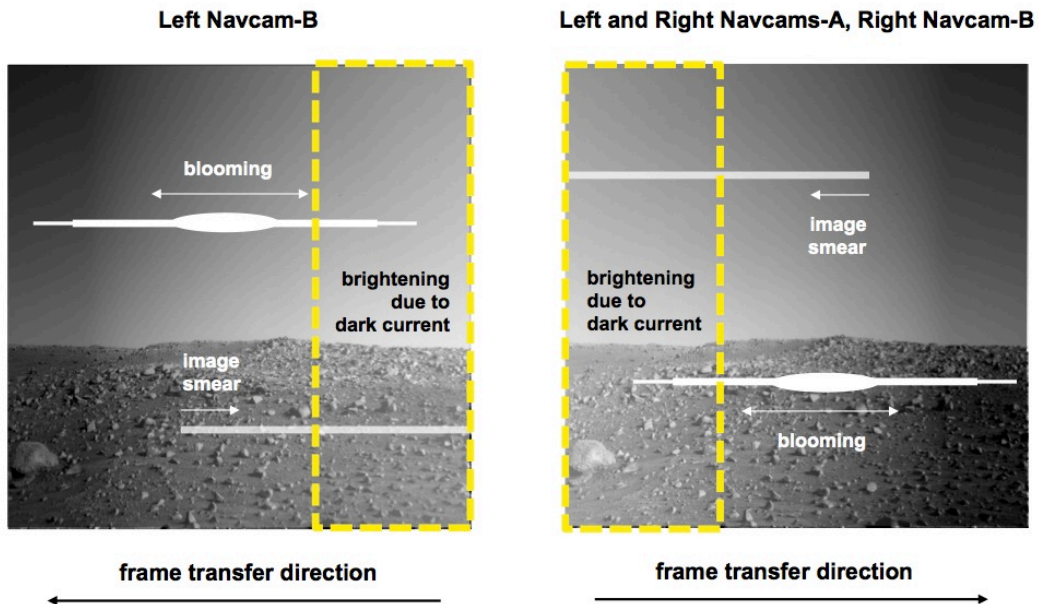


**Figure 7. Clocking effects on the appearance of Navcam images**

#### 2.1.1.4 Navcam Pointing

Transformations for pointing the Navcams are presented in Section 2.2.1.3.

#### 2.1.1.5 Hazcam Description

MSL has eight Hazcams: left and right front Hazcams A form the primary forward-facing stereo pair, mounted on the front of the chassis and connected to Rover Compute Element A (RCE-A); left and right rear Hazcams A form the primary rearward-facing stereo pair, mounted on the rear of the chassis on the -Y side of the RTG and connected to Rover Compute Element A (RCE-A); left and right front Hazcams B form a backup forward-facing stereo pair, mounted on the front of the chassis and connected to Rover Compute Element B (RCE-B); and left and right rear Hazcams B form a backup rearward-facing stereo pair, mounted on the rear of the chassis on the +Y side of the RTG and connected to Rover Compute Element B (RCE-B). The designations left and right are with respect to the viewing direction.

Each Hazcam has a 120° field-of-view (FOV) f-theta lens and a 1024x1024 pixel detector array.

Hazcam images are used by operators on the ground to view the terrain around the rover, and are used both in onboard and ground-based stereo image processing to derive range maps of the surface. These range data are used for mobility hazard detection and for determination of the location of the surface in the sample acquisition workspace in support of surface contact operations.

The locations of the front and rear Hazcams are shown in Figure 8, Figure 10, and Figure 11.

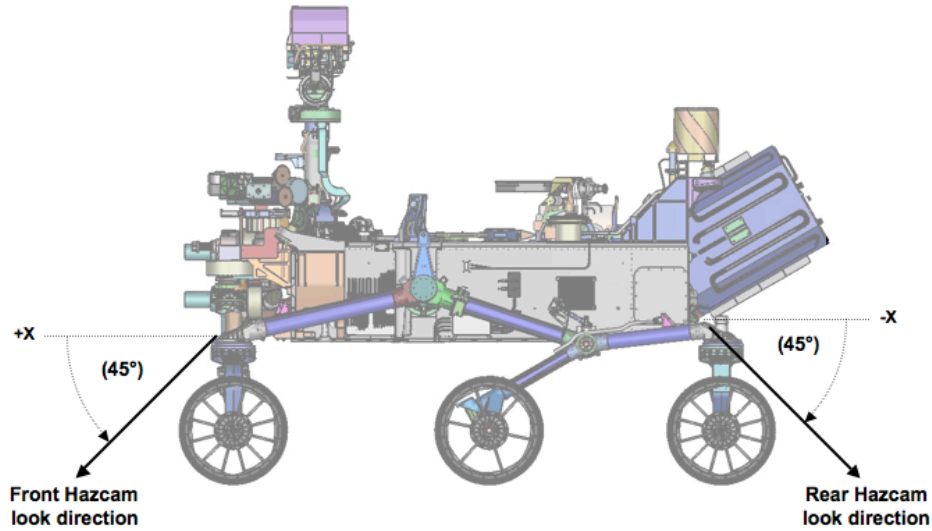


Figure 8. Locations of the Hazcams -- side view

#### 2.1.1.6 Hazcam Clocking

Each precise Hazcam "boresight" orientation is determined by camera calibration procedures performed in ATLO, and is embodied in a camera model which provides mapping between the vectors from each of the pixels of the camera out into the world, with reference to a fixed rover frame, measured with respect to datum points and/or secondary fiducials.

Hazcam frame transfer directions are shown in Figure 9, Figure 10, and Figure 11. Frame transfer direction is shown relative to the camera CCD.

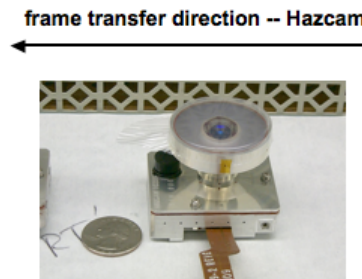
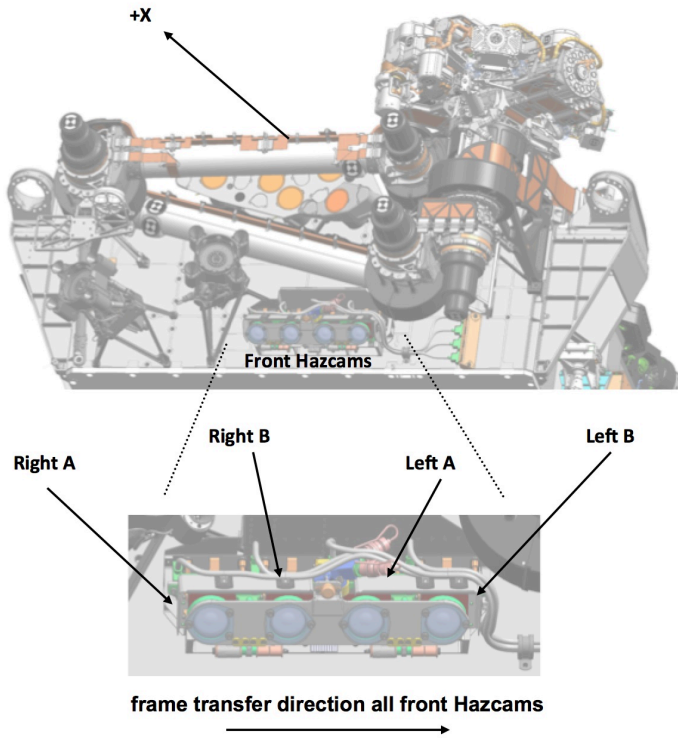
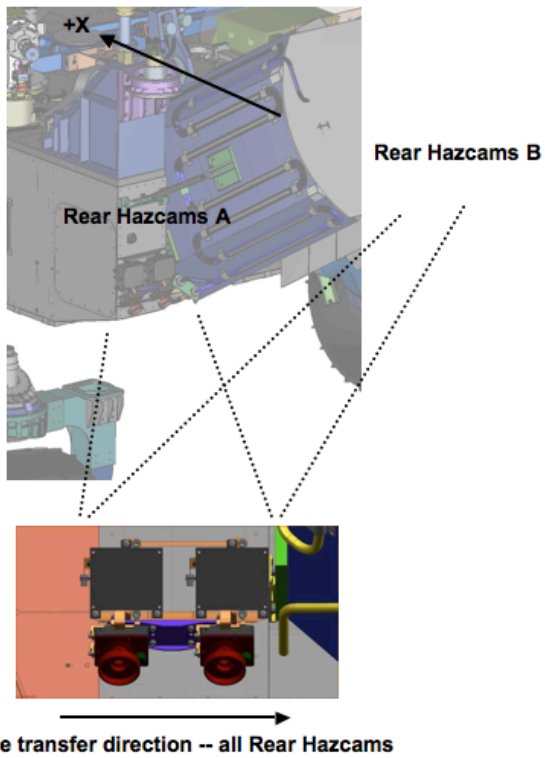


Figure 9. Hazcam frame transfer direction



**Figure 10. Front Hazcam locations and frame transfer directions as mounted**



**Figure 11. Rear Hazcam locations and frame transfer directions as mounted**

The effects of clocking on the appearance of Hazcam images are shown in Figure 12.

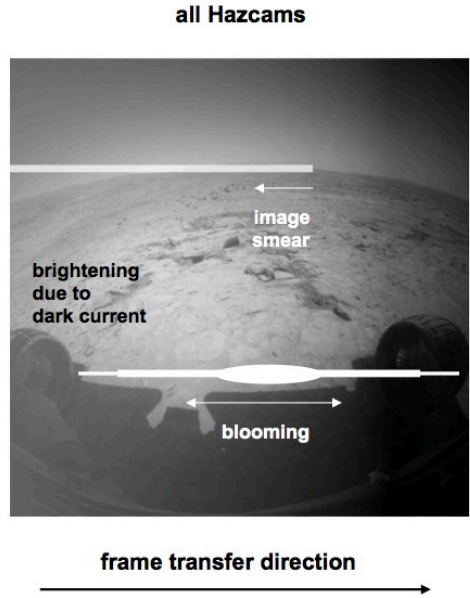


**Figure 12. Clocking effects on the appearance of Hazcam images**

**2.1.1.7 Hazcam Pointing**

Table 1 lists the set of Hazcam names.

**Table 1. Hazcam names**

<b>Hazcam</b>	<b>Designation</b>	<b>Frame Manager Name</b>
left eye front Hazcam (A-side)	lfha	(none)
right eye front Hazcam (A-side)	rfha	(none)
left eye front Hazcam (B-side)	lfhb	(none)
right eye front Hazcam (B-side)	rfhb	(none)
left eye rear Hazcam (A-side)	lrha	(none)
right eye rear Hazcam (A-side)	rrha	(none)
left eye rear Hazcam (B-side)	lrhb	(none)
right eye rear Hazcam (B-side)	rrhb	(none)

The locations  $(x,y,z)$  and orientations  $(\phi_z, \phi_y)$  of the Hazcams as mounted on the rover chassis are presented in Table 2. Designations left and right for each stereo pair are relative to the viewing direction.

**Table 2. Translational and angular offsets relating Hazcam boresight vectors to the rover mechanical frame**

<b>Boresight</b>	<b>Reference Frame</b>	<b>Names</b>	<b>Translational and Angular Offsets to the Boresight Vector</b>		
left eye front Hazcam (A-Side)	RM	${}^{RM}T^{LFHA}$	X	(947.44)	mm
			Y	(-87.95)	mm
			Z	(416.10)	mm
			$\phi_z$	(0)	°
			$\phi_y$	(-45)	°
			in rover mechanical frame		

right eye front Hazcam (A-Side)	RM	$RM_{T^{RFHA}}$	X (947.44) mm Y (78.35) mm Z (416.10) mm $\varphi_Z$ (0) ° $\varphi_Y$ (-45) ° in rover mechanical frame
left eye front Hazcam (B-Side)	RM	$RM_{T^{LFHB}}$	X (947.44) mm Y (-171.10) mm Z (416.10) mm $\varphi_Z$ (0) ° $\varphi_Y$ (-45) ° in rover mechanical frame
right eye front Hazcam (B-Side)	RM	$RM_{T^{RFHB}}$	X (947.44) mm Y (-4.80) mm Z (416.10) mm $\varphi_Z$ (0) ° $\varphi_Y$ (-45) ° in rover mechanical frame
left eye rear Hazcam (A-Side)	RM	$RM_{T^{LRHA}}$	X (-1069.93) mm Y (-456.19) mm Z (344.50) mm $\varphi_Z$ (180) ° $\varphi_Y$ (-45) ° in rover mechanical frame
right eye rear Hazcam (A-Side)	RM	$RM_{T^{RRHA}}$	X (-1069.93) mm Y (-556.19) mm Z (344.50) mm $\varphi_Z$ (180) ° $\varphi_Y$ (-45) ° in rover mechanical frame
left eye rear Hazcam (B-Side)	RM	$RM_{T^{LRHB}}$	X (-1069.93) mm Y (551.75) mm Z (344.50) mm $\varphi_Z$ (180) ° $\varphi_Y$ (-45) ° in rover mechanical frame
right eye rear Hazcam (B-Side)	RM	$RM_{T^{RRHB}}$	X (-1069.93) mm Y (451.75) mm Z (344.50) mm $\varphi_Z$ (180) ° $\varphi_Y$ (-45) ° in rover mechanical frame

For all eight Hazcams, the calibrated location and direction of each boresight is embodied within its camera model determined in ATLO.

### 2.1.2 ChemCam and Mastcam Pointing

Pointing for the ChemCam and Mastcams is presented in Section 2.2.1.3.

### 2.1.3 MARDI Pointing

The location  $(x,y,z)$  and orientation  $(\phi_Z, \phi_Y)$  of MARDI as mounted on the rover chassis are presented in Table 3.

**Table 3. Translational and angular offsets relating the MARDI boresight to the rover mechanical frame**

<b>Boresight</b>	<b>Reference Frame</b>	<b>Names</b>	<b>Translational and Angular Offsets to the Boresight Vector</b>		
MARDI	RM	${}_{RM}T^{MARDI}$	X	(671.26)	mm
			Y	(-647.80)	mm
			Z	(456.22)	mm
			$\phi_Z$	(0)	°
			$\phi_Y$	(-90)	°
			in rover mechanical frame		

The calibrated location and direction of MARDI's boresight is embodied within its camera model determined in ATLO.

### 2.1.4 RAD and REMS Pointing

The locations  $(x,y,z)$  and orientations  $(\phi_Z, \phi_Y)$  of the RAD and REMS sensors as mounted on the rover after the RSM is deployed are presented in Table 4.

**Table 4. Translational and angular offsets relating RAD and REMS sensor orientation to the rover mechanical frame**

<b>Boresight</b>	<b>Reference Frame</b>	<b>Names</b>	<b>Translation and Angular Offsets to the Boresight</b>
RAD	RM	${}_{RM}T^{RAD}$	X (74.60) mm Y (-353.00) mm Z (-15.00) mm $\varphi_Z$ (0) ° $\varphi_Y$ (+90) ° in rover mechanical frame
REMS UV	RM	${}_{RM}T^{REMS-UV}$	X (515.59) mm Y (246.47) mm Z (-23.50) mm $\varphi_Z$ (0) ° $\varphi_Y$ (+90) ° in rover mechanical frame
tip of REMS BOOM 1	RM	${}_{RM}T^{REMS-BOOM1}$	X (605.74) mm Y (732.28) mm Z (-425.65) mm $\varphi_Z$ (+90) ° $\varphi_Y$ (0) ° in rover mechanical frame
tip of REMS BOOM 2	RM	${}_{RM}T^{REMS-BOOM2}$	X (918.12) mm Y (566.18) mm Z (-392.65) mm $\varphi_Z$ (0) ° $\varphi_Y$ (0) ° in rover mechanical frame

### 2.1.5 Chassis-mounted Fiducial Locations

There are ten fiducials mounted in fixed relationship to the rover chassis: five on the top deck, two on the rear wheel restraints, and three on the Organic Check Material (OCM) assembly. These are shown in Figure 13 and Figure 14.

The locations (x,y,z) of the centers of these fiducials are presented in Table 5.

The locations of deck and wheel restraint fiducials, which were not present in CAD models, are derived from ATLO metrology; the locations of OCM fiducials are derived from CAD models.

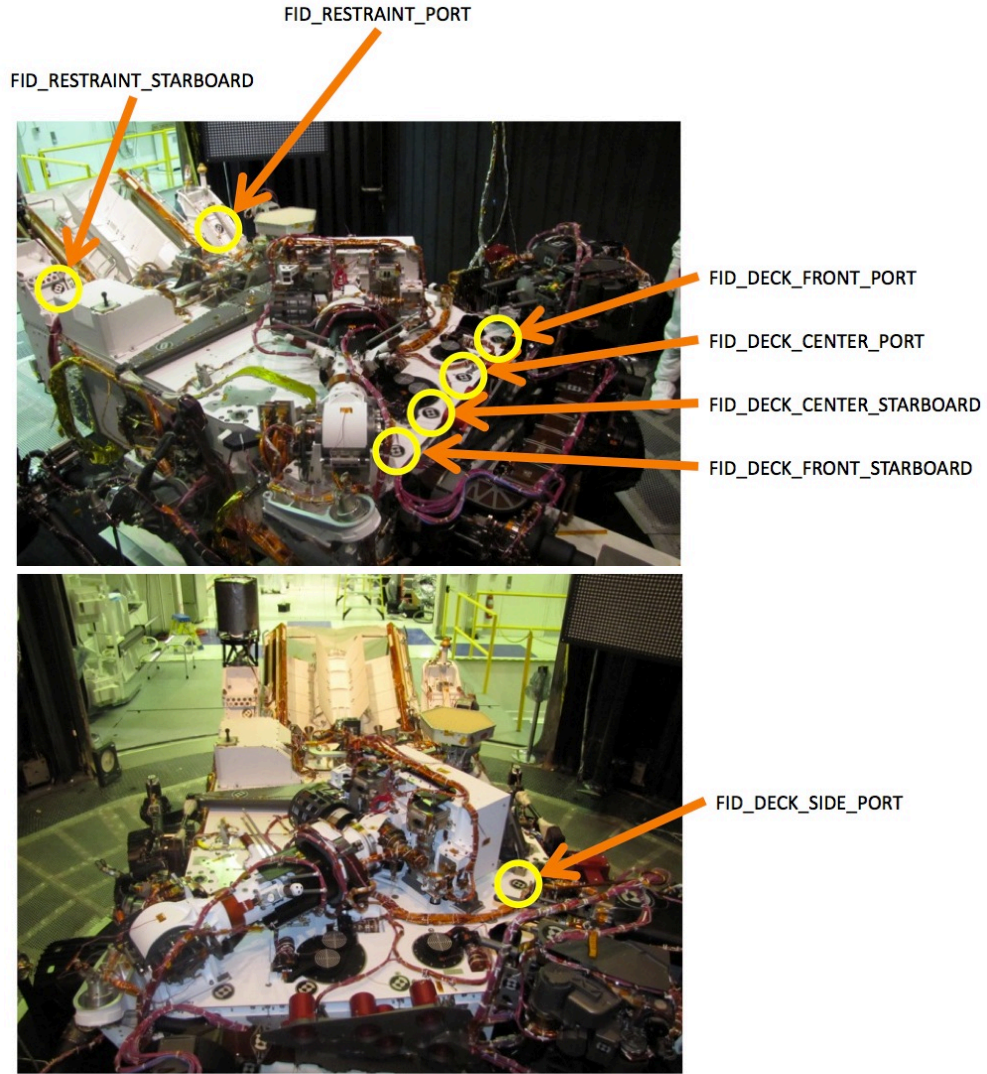


Figure 13. Deck and wheel restraint fiducials

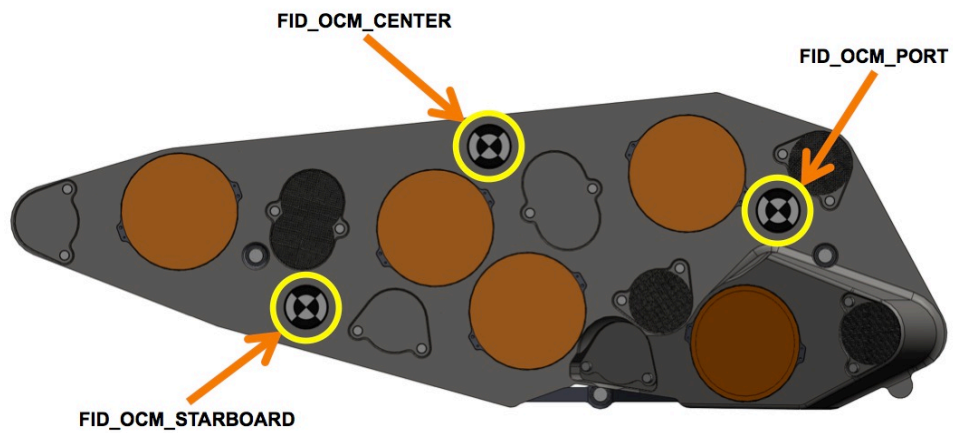


Figure 14. OCM fiducials

**Table 5. Translational offsets relating chassis-mounted fiducials to the rover mechanical frame**

<b>Fiducial</b>	<b>Reference Frame</b>	<b>Names</b>	<b>Translational Offsets to the Fiducial</b>
RESTRAINT_PORT	RM	$RM_{T}RESTRAINT\_PORT$	X     -824.86     mm Y     -466.12     mm Z     -127.65     mm in rover mechanical frame
RESTRAINT_STARBOARD	RM	$RM_{T}RESTRAINT\_STARBOARD$	X     -824.63     mm Y     467.35     mm Z     -128.13     mm in rover mechanical frame
DECK_SIDE_PORT	RM	$RM_{T}DECK\_SIDE\_PORT$	X     409.27     mm Y     -442.40     mm Z     -0.38     mm in rover mechanical frame
DECK_FRONT_PORT	RM	$RM_{T}DECK\_FRONT\_PORT$	X     782.01     mm Y     -302.67     mm Z     -0.67     mm in rover mechanical frame
DECK_CENTER_PORT	RM	$RM_{T}DECK\_CENTER\_PORT$	X     782.02     mm Y     -1.05     mm Z     -0.62     mm in rover mechanical frame
DECK_CENTER_STARBOARD	RM	$RM_{T}DECK\_CENTER\_STARBOARD$	X     782.16     mm Y     229.15     mm Z     -0.47     mm in rover mechanical frame
DECK_FRONT_STARBOARD	RM	$RM_{T}DECK\_FRONT\_STARBOARD$	X     782.36     mm Y     431.78     mm Z     -0.39     mm in rover mechanical frame
OCM_PORT	RM	$RM_{T}OCM\_PORT$	X     (931.85)     mm Y     (-93.57)     mm Z     (-16.41)     mm in rover mechanical frame
OCM_CENTER	RM	$RM_{T}OCM\_CENTER$	X     (931.85)     mm Y     (66.53)     mm Z     (-53.35)     mm in rover mechanical frame
OCM_STARBOARD	RM	$RM_{T}OCM\_STARBOARD$	X     (931.85)     mm Y     (169.15)     mm Z     (35.59)     mm in rover mechanical frame

## 2.2 Actuators

Flight software commands actuators for mobility and for RSM and HGA pointing. It also monitors the mobility suspension sensors to determine the configuration of the passive suspension system. The phasing of RSM and mobility actuators at the operations and command levels is presented here. Ranges of motion are also included as appropriate.

### 2.2.1 Remote Sensing Mast (RSM)

#### 2.2.1.1 The RSM Elevation Actuator

For the RSM elevation actuator,  $0^\circ$  in joint angles is defined as the configuration when the actuator is against the hard stop and the mast-mounted instruments would be looking in the direction of the base of the mast.

All elevation joint angles are positive, defined relative to this hard stop. Note that motion to the lower elevation hard stop is restricted, to avoid hardware damage.

The second hard stop prevents positive actuator motion beyond  $[182^\circ]$  elevation joint angle.

The elevation joint angle at which the ChemCam and Navcam boresight vectors lie in a horizontal plane (parallel to the rover mechanical X-Y plane) will be measured in ATLO. This zero offset value is used in the calculation of kinematics for pointing relative to the rover mechanical frame (see section 2.2.1.3, below).

These are illustrated in Figure 15.

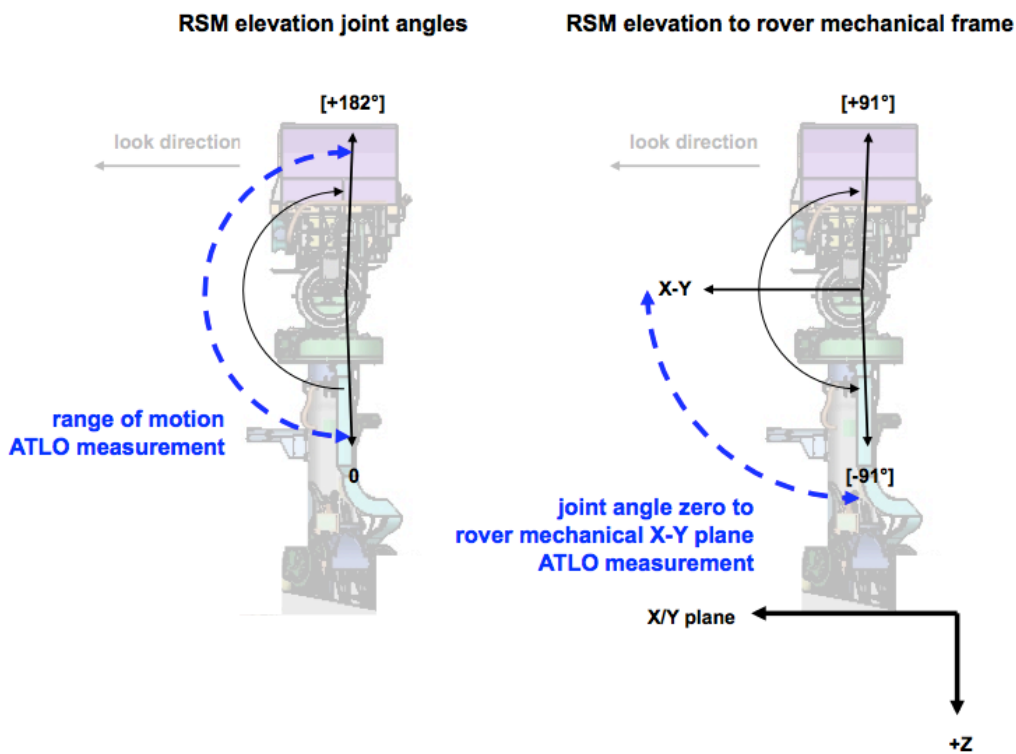


Figure 15. RSM elevation actuator joint angles

#### 2.2.1.2 The RSM Azimuth Actuator

For the RSM azimuth actuator,  $0^\circ$  in joint angles is defined as the configuration when the actuator is against the hard stop preventing mast-mounted instruments from rotating further to the left, when the camera plate is horizontal and the ChemCam is on top (counter-clockwise when viewed from above, negative direction about rover mechanical positive Z).

All azimuth joint angles are positive, measured away from this hard stop.

The second hard stop prevents positive actuator motion beyond  $[362^\circ]$  to the right.

The azimuth joint angle at which the ChemCam and Navcam boresight vectors lie in vertical planes parallel to the rover mechanical X-Z plane will be measured in ATLO. This zero offset value is used in the calculation of kinematics for pointing relative to the rover mechanical frame (see section 2.2.1.3, below).

These are illustrated in Figure 16.

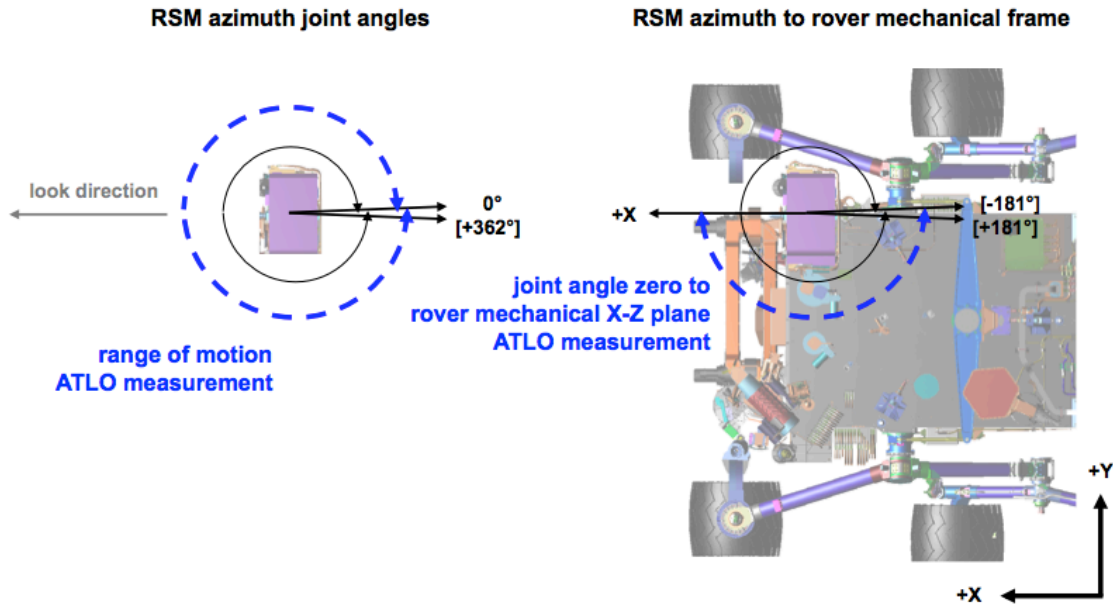


**Figure 16. RSM azimuth actuator joint angles**

### 2.2.1.3 RSM Forward Kinematics and Pointing

(Note that flight and ground software may implement different, but mathematically equivalent, representations of RSM kinematics.)

Pointing of RSM-mounted instruments relative to the rover mechanical frame can be described mathematically by attaching coordinate systems to the azimuth and elevation joints, and then specifying boresight vectors relative to the elevation joint. Since all pointing is performed after RSM deployment, and since all calibrations are also made after deployment, only the azimuth and elevation joints are needed in the kinematic model.

We locate the origin of the RSM azimuth frame at the point where the azimuth axis intersects the elevation axis (or the nearest point if ATLO measurements show them not to intersect). Positive Z points down, along the azimuth axis, in the direction of positive Z of the rover mechanical frame. Positive X points in the direction of the ChemCam and Navcam boresights when the elevation axis points them in the horizontal plane (the Mastcams are toed-in). Positive Y completes the right-handed coordinate system.

We locate the origin of the RSM elevation frame at the point where the elevation axis intersects the azimuth axis (or the nearest point if ATLO measurements show them not to intersect). Positive Z points along the elevation axis, in the direction of azimuth positive Y. Positive X points in the direction of the Chemcam and Navcam boresights. Positive Y completes the right-handed coordinate system.

Table 6 lists the set of RSM instrument pointing frames and vectors.

**Table 6. RSM pointing frame and vector names**

Frame or Vector	Designation	Frame Manager Name
rover mechanical	rm	RMECH
RSM azimuth	maz	(none)
RSM elevation	mel	(none)

ChemCam RMI	rmi	RMI
ChemCam LIBS	libs	LIBS
left Mastcam	lmc	MCAML
right Mastcam	rmc	MCAMR
left Navcam A-side	lna	NCAML
right Navcam A-side	rna	NCAMR
left Navcam B-side	lnb	NCAML
right Navcam B-side	rnb	NCAMR

Figure 17 shows the RSM frames for the ChemCam boresight. This pattern applies for all other boresights.

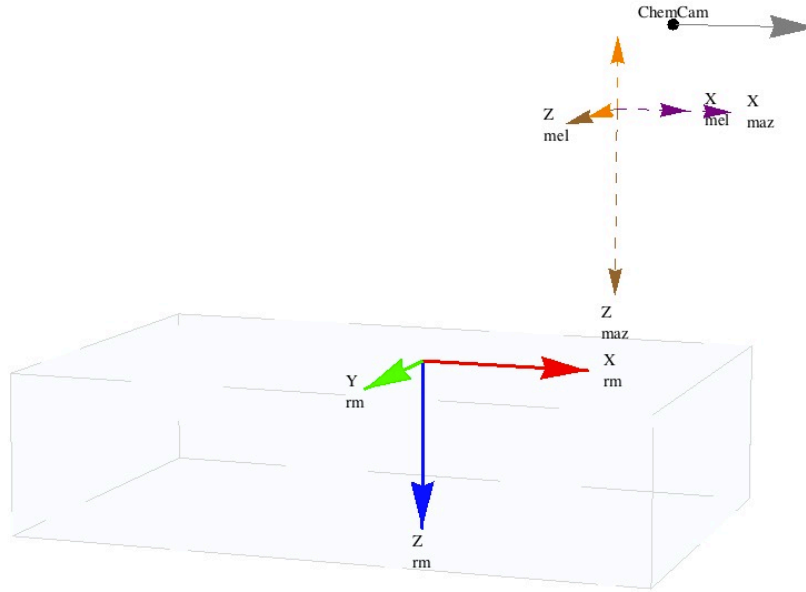


**Figure 17. RSM azimuth and elevation coordinate frames relative to the rover mechanical frame and the ChemCam boresight when pointing straight forward**

Rotation and translation matrices for the RSM azimuth and elevation actuators after RSM deployment are presented in Table 7 and Table 8.

**Table 7. Rotation matrices relating RSM azimuth and elevation actuator frames to their parent frames**

Frame	Names	Direction Cosine Matrices		
RSM azimuth	$RM_{C^{MAZ}}$	$\cos(\theta_{maz} + [-181]^\circ)$	$-\sin(\theta_{maz} + [-181]^\circ)$	0
		$\sin(\theta_{maz} + [-181]^\circ)$	$\cos(\theta_{maz} + [-181]^\circ)$	0
		0	0	1
RSM elevation	$MAZ_{C^{MEL}}$	$\cos(\theta_{mel} + [-91]^\circ)$	$-\sin(\theta_{mel} + [-91]^\circ)$	0
		0	0	1
		$-\sin(\theta_{mel} + [-91]^\circ)$	$-\cos(\theta_{mel} + [-91]^\circ)$	0

**Table 8. Translational offsets relating RSM azimuth and elevation actuator frames to their parent frames**

Joint Frame	Reference Frame	Names	Translation Offset to the Origin of the Joint Frame
RSM azimuth	RM	$RM_T^{MAZ}$	X [713.98] mm Y [559.05] mm Z [-785.89] mm in rover mechanical frame
RSM elevation	RSM azimuth	$MAZ_T^{MEL}$	X [0] mm Y [0] mm Z [0] mm in RSM azimuth frame

We specify the boresight vector for each of the RSM-mounted instruments relative to the elevation joint frame with five values: a translational offset (x,y,z) plus rotations ( $\phi_Z, \phi_Y$ ) in order about the elevation joint frame Z and Y axes. These are presented in Table 9.

**Table 9. Translational and angular offsets relating RSM boresight vectors to the RSM elevation frame**

Boresight	Reference Frame	Names	Translation and Angular Offsets to the Boresight
ChemCam RMI	RSM elevation	$MEL_T^{RMI}$	X [117.23] mm Y [213.61] mm Z [-112.09] mm $\phi_Z$ [0] ° $\phi_Y$ [0] ° in RSM elevation frame
ChemCam LIBS	RSM elevation	$MEL_T^{LIBS}$	X [117.23] mm Y [213.61] mm Z [-112.09] mm $\phi_Z$ [0] ° $\phi_Y$ [0] ° in RSM elevation frame
left Mastcam	RSM elevation	$MEL_T^{LMC}$	X (77.74) mm Y (65.27) mm Z (-125.11) mm $\phi_Z$ (0) ° $\phi_Y$ (-1.25) ° in RSM elevation frame
right Mastcam	RSM elevation	$MEL_T^{RMC}$	X (77.74) mm Y (65.27) mm Z (120.06) mm $\phi_Z$ (0) ° $\phi_Y$ (1.25) ° in RSM elevation frame

upper left Navcam (A-Side)	RSM elevation	$MEL_T^{LNA}$	X (139.43) mm Y (82.00) mm Z (-214.39) mm $\phi_Z$ (0) ° $\phi_Y$ (0) ° in RSM elevation frame
upper right Navcam (A-Side)	RSM elevation	$MEL_T^{RNA}$	X (139.43) mm Y (82.00) mm Z (209.61) mm $\phi_Z$ (0) ° $\phi_Y$ (0) ° in RSM elevation frame
lower left Navcam (B-Side)	RSM elevation	$MEL_T^{LNB}$	X (139.43) mm Y (33.96) mm Z (-214.39) mm $\phi_Z$ (0) ° $\phi_Y$ (0) ° in RSM elevation frame
lower right Navcam (B-Side)	RSM elevation	$MEL_T^{RNB}$	X (139.43) mm Y (33.96) mm Z (209.61) mm $\phi_Z$ (0) ° $\phi_Y$ (0) ° in RSM elevation frame

For the ChemCam, both Mastcams, and all four Navcams, the calibrated direction of each boresight is embodied within its camera model determined in ATLO. The as-designed values of  $\phi_Z$  and  $\phi_Y$  are presented here.

Figure 18 shows the frame tree for pointing RSM instruments. Red indicates articulated joints.

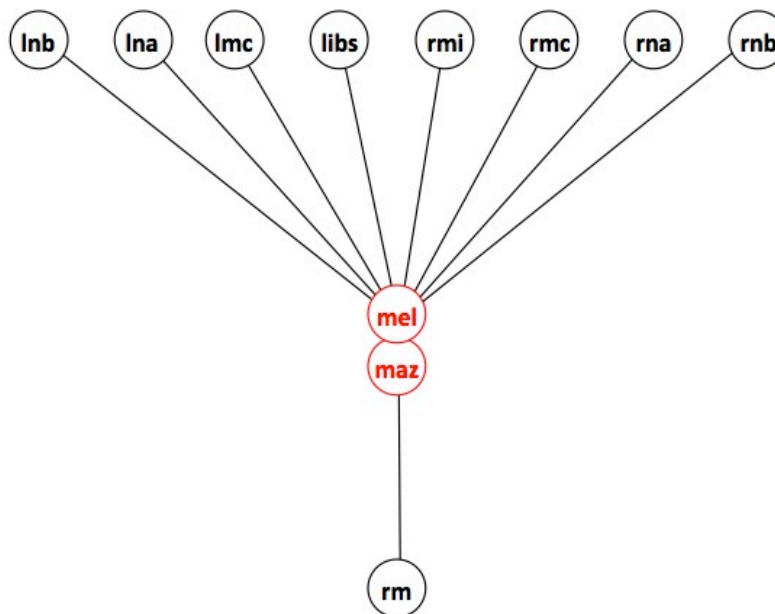


**Figure 18. The frame tree for RSM pointing**

The location of each boresight in the rover mechanical frame for any pair of RSM joint angles  $\theta_{maz}$  and  $\theta_{mel}$ , is given by the expression

$${}^{RM}C^{MAZ} \cdot ({}^{MAZ}C^{MEL} \cdot {}^{MEL}T^{boresight} + {}^{MAZ}T^{MEL}) + {}^{RM}T^{MAZ}$$

where  ${}^{RM}C^{MAZ}$  and  ${}^{MAZ}C^{MEL}$  are from Table 7,  ${}^{RM}T^{MAZ}$  and  ${}^{MAZ}T^{MEL}$  from Table 8, and  ${}^{MEL}T^{boresight}$  for each boresight from Table 9 above.

The unit vector pointing in the view direction of each boresight is given by

$${}^{RM}C^{MAZ} \cdot {}^{MAZ}C^{MEL} \cdot {}^{MEL}U^{boresight}$$

where the unit vector  ${}^{MEL}U^{boresight}$  is derived from offset angles  $\phi_Z$  and  $\phi_Y$  for that boresight from Table 9 as given in Table 10.

**Table 10. The boresight unit vector in the RSM elevation frame**

Boresight	Reference Frame	Names	Unit Vector Components												
boresight	RSM elevation	${}^{MEL}U^{boresight}$	<table style="border: none;"> <tr> <td>X</td> <td><math>\cos(\phi_Z) \cos(\phi_Y)</math></td> <td>mm</td> </tr> <tr> <td>Y</td> <td><math>\sin(\phi_Z) \cos(\phi_Y)</math></td> <td>mm</td> </tr> <tr> <td>Z</td> <td><math>-\sin(\phi_Y)</math></td> <td>mm</td> </tr> <tr> <td colspan="3" style="text-align: center;">in RSM elevation frame</td> </tr> </table>	X	$\cos(\phi_Z) \cos(\phi_Y)$	mm	Y	$\sin(\phi_Z) \cos(\phi_Y)$	mm	Z	$-\sin(\phi_Y)$	mm	in RSM elevation frame		
X	$\cos(\phi_Z) \cos(\phi_Y)$	mm													
Y	$\sin(\phi_Z) \cos(\phi_Y)$	mm													
Z	$-\sin(\phi_Y)$	mm													
in RSM elevation frame															

#### 2.2.1.4 Calibration Targets for RSM Instruments

There are two calibration targets for RSM-mounted instruments installed on the rover chassis: the ChemCam calibration target and the Mastcam calibration target.

The ChemCam calibration target contains two rows of calibration disks, with five in the upper row and four in the lower row. There is also a square at the end of the lower row of disks. The vectors presented here are normal to the target, pointing at the center of each disk and at the center of the square.

The Mastcam calibration target is mounted horizontally, with a sphere mounted on an upward projecting post. The vector presented here is pointing downward at the center of the sphere.

Figure 19 shows the ChemCam calibration target.

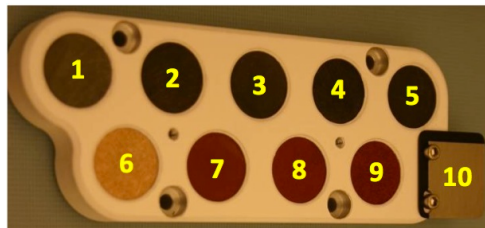


**Figure 19. The ChemCam calibration target**

Figure 20 shows the Mastcam calibration target.



**Figure 20. The Mastcam calibration target**

Table 11 lists the set of calibration targets for RSM instruments.

**Table 11. RSM calibration target names**

Target	Designation	Frame Manager Name
upper left ChemCam calibration target disk	ct1	CCAM_CAL1
upper middle left ChemCam calibration target disk	ct2	CCAM_CAL2
upper middle ChemCam calibration target	ct3	CCAM_CAL3
upper middle right ChemCam calibration target disk	ct4	CCAM_CAL4
upper right ChemCam calibration target disk	ct5	CCAM_CAL5
lower left ChemCam calibration target disk	ct6	CCAM_CAL6
lower middle left ChemCam calibration target disk	ct7	CCAM_CAL7
lower middle right ChemCam calibration target disk	ct8	CCAM_CAL8
lower right ChemCam calibration target disk	ct9	CCAM_CAL9
lower far right ChemCam calibration target square	ct10	CCAM_CAL10
Mastcam calibration target	mt	MCAM_CAL

Table 12 presents RSM instrument calibration target locations and normal vectors.

**Table 12. Translational and angular offsets relating RSM calibration target normal vectors to the rover mechanical frame**

Normal to Target	Reference Frame	Names	Translation and Angular Offsets into the Target Normal															
upper left ChemCam calibration target disk	RM	$RM_{T^{CT1}}$	<table> <tr><td>X</td><td>[-850.21]</td><td>mm</td></tr> <tr><td>Y</td><td>[557.54]</td><td>mm</td></tr> <tr><td>Z</td><td>[-190.62]</td><td>mm</td></tr> <tr><td><math>\varphi_Z</math></td><td>[180]</td><td>°</td></tr> <tr><td><math>\varphi_Y</math></td><td>[-37.9]</td><td>°</td></tr> </table> <p>in rover mechanical frame</p>	X	[-850.21]	mm	Y	[557.54]	mm	Z	[-190.62]	mm	$\varphi_Z$	[180]	°	$\varphi_Y$	[-37.9]	°
X	[-850.21]	mm																
Y	[557.54]	mm																
Z	[-190.62]	mm																
$\varphi_Z$	[180]	°																
$\varphi_Y$	[-37.9]	°																
upper middle left ChemCam calibration target disk	RM	$RM_{T^{CT2}}$	<table> <tr><td>X</td><td>[-850.21]</td><td>mm</td></tr> <tr><td>Y</td><td>[531.35]</td><td>mm</td></tr> <tr><td>Z</td><td>[-190.62]</td><td>mm</td></tr> <tr><td><math>\varphi_Z</math></td><td>[180]</td><td>°</td></tr> <tr><td><math>\varphi_Y</math></td><td>[-37.9]</td><td>°</td></tr> </table> <p>in rover mechanical frame</p>	X	[-850.21]	mm	Y	[531.35]	mm	Z	[-190.62]	mm	$\varphi_Z$	[180]	°	$\varphi_Y$	[-37.9]	°
X	[-850.21]	mm																
Y	[531.35]	mm																
Z	[-190.62]	mm																
$\varphi_Z$	[180]	°																
$\varphi_Y$	[-37.9]	°																
upper middle ChemCam calibration target	RM	$RM_{T^{CT3}}$	<table> <tr><td>X</td><td>[-850.21]</td><td>mm</td></tr> <tr><td>Y</td><td>[505.15]</td><td>mm</td></tr> <tr><td>Z</td><td>[-190.62]</td><td>mm</td></tr> <tr><td><math>\varphi_Z</math></td><td>[180]</td><td>°</td></tr> <tr><td><math>\varphi_Y</math></td><td>[-37.9]</td><td>°</td></tr> </table> <p>in rover mechanical frame</p>	X	[-850.21]	mm	Y	[505.15]	mm	Z	[-190.62]	mm	$\varphi_Z$	[180]	°	$\varphi_Y$	[-37.9]	°
X	[-850.21]	mm																
Y	[505.15]	mm																
Z	[-190.62]	mm																
$\varphi_Z$	[180]	°																
$\varphi_Y$	[-37.9]	°																

upper middle right ChemCam calibration target disk	RM	$RM_{T^{CT4}}$	X [-850.21] mm Y [478.96] mm Z [-190.62] mm $\varphi_Z$ [180] ° $\varphi_Y$ [-37.9] ° in rover mechanical frame
upper right ChemCam calibration target disk	RM	$RM_{T^{CT5}}$	X [-850.21] mm Y [452.77] mm Z [-190.62] mm $\varphi_Z$ [180] ° $\varphi_Y$ [-37.9] ° in rover mechanical frame
lower left ChemCam calibration target disk	RM	$RM_{T^{CT6}}$	X [-836.56] mm Y [544.45] mm Z [-173.09] mm $\varphi_Z$ [180] ° $\varphi_Y$ [-37.9] ° in rover mechanical frame
lower middle left ChemCam calibration target disk	RM	$RM_{T^{CT7}}$	X [-836.56] mm Y [518.25] mm Z [-173.09] mm $\varphi_Z$ [180] ° $\varphi_Y$ [-37.9] ° in rover mechanical frame
lower middle right ChemCam calibration target disk	RM	$RM_{T^{CT8}}$	X [-836.56] mm Y [492.06] mm Z [-173.09] mm $\varphi_Z$ [180] ° $\varphi_Y$ [-37.9] ° in rover mechanical frame
lower right ChemCam calibration target disk	RM	$RM_{T^{CT9}}$	X [-836.56] mm Y [465.86] mm Z [-173.09] mm $\varphi_Z$ [180] ° $\varphi_Y$ [-37.9] ° in rover mechanical frame
lower far right ChemCam calibration target square	RM	$RM_{T^{CT10}}$	X [-835.58] mm Y [438.48] mm Z [-171.83] mm $\varphi_Z$ [180] ° $\varphi_Y$ [-37.9] ° in rover mechanical frame

Mastcam calibration target (center of sphere)	RM	${}^{RM}_T{}^{MT}$	X	[-375.20]	mm
			Y	[514.01]	mm
			Z	[-218.89]	mm
			$\varphi_Z$	0	°
			$\varphi_Y$	-90	°
			in rover mechanical frame		

RSM joint angles for pointing the ChemCam laser at the ChemCam calibration target will be directly determined in ATLO, so specific metrology of the location of the ChemCam calibration target is not needed.

## 2.2.2 Mobility

### 2.2.2.1 Steering Actuators

The rover has four-wheel steering.

For each of the four steering actuators,  $0^\circ$  joint angle is defined as the configuration where the axis of its wheel is parallel to the Rover Mechanical Frame Y vector, aligned for driving straight forward (or backward).

Negative steering angle is measured from  $0^\circ$  to the left, toward the direction of the -Y axis of the Rover Mechanical Frame.

Positive steering angle is measured from  $0^\circ$  to the right, toward the direction of the +Y axis of the Rover Mechanical Frame.

Mechanical hard stops prevent negative and positive steering actuator motion beyond  $[-90^\circ]$  and  $[+90^\circ]$  respectively.

For driving arcs to the right, the front steering actuators are set to positive angles and the rear steering actuators are set to negative angles.

For driving arcs to the left, the front steering actuators are set to negative angles and the rear steering actuators are set to positive angles.

For turning in place, the right front and left rear steering actuators are set to negative angles and the left front and right rear steering actuators are set to positive angles.

Phasing of the steering actuators is illustrated in Figure 21.

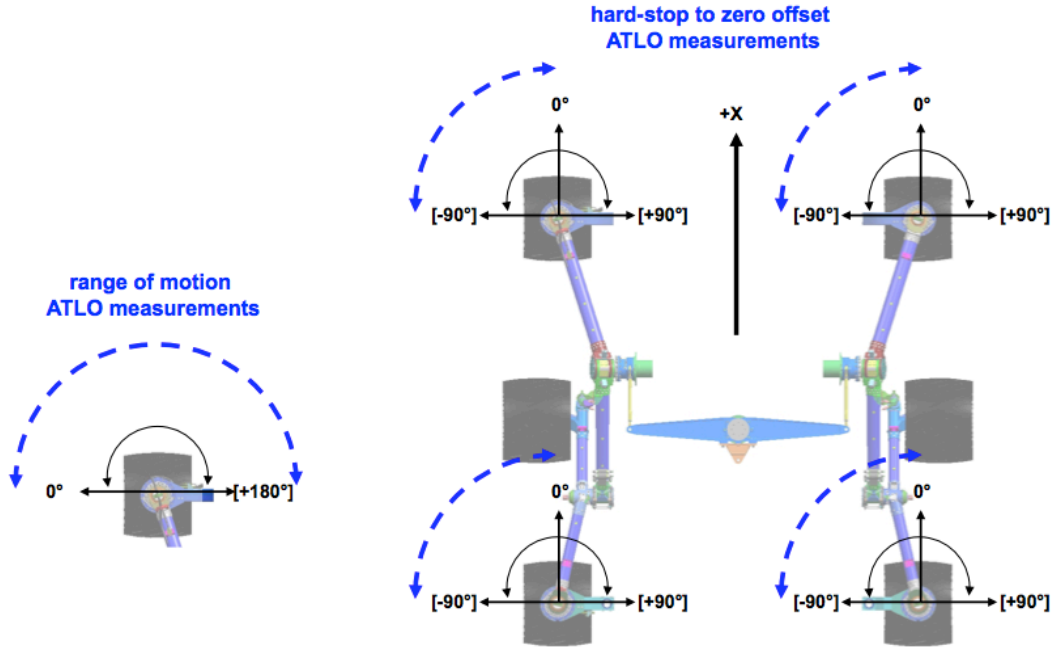


**Figure 21. Steering direction**

**2.2.2.2 Drive Actuators**

For all six wheels of the rover, positive drive rotation is the direction for forward vehicle motion (in the direction of the Rover Mechanical Frame +X vector), and negative drive rotation is the direction for backward vehicle motion.

Drive rotation is relative: there is no 0° angular origin.

Phasing of the drive actuators is illustrated in Figure 22.

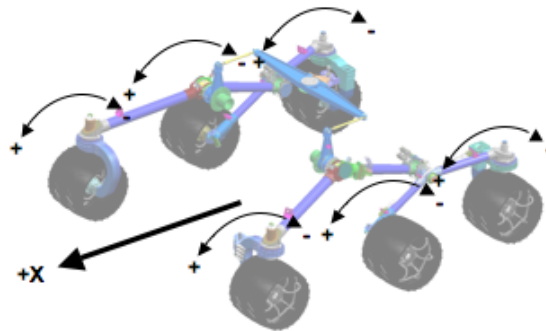


**Figure 22. Drive direction**

**2.2.2.3 Passive Suspension Sensors**

The mobility system has a three degree-of-freedom suspension system which passively complies to maintain contact between each of the six wheels and the surface, while at the same time minimizing rover body tilt. Elements of this passive suspension system are a differential, left and right rockers, and left and right bogies, shown in Figure 23.

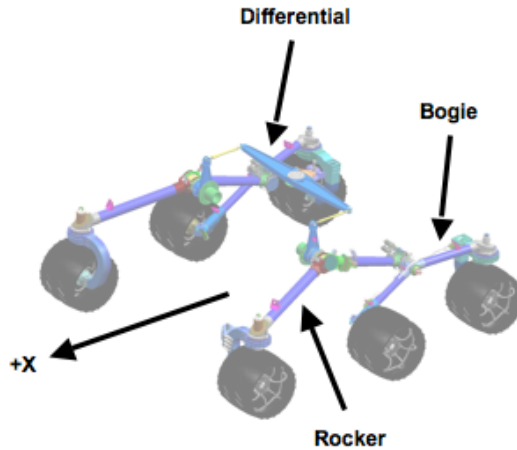


**Figure 23. The mobility suspension system**

The differential and rockers are mechanically linked so that left and right front wheels move vertically equal amounts but in the opposite directions with respect to the rover deck: When the left front wheel moves up, the right front wheel moves down by the same amount. This constitutes one degree of freedom, which is redundantly measured with absolute angle position sensor on each rocker.

The 0° point for both rockers corresponds to the state of the differential/rockers when the vehicle sits on a flat horizontal surface. For each rocker, positive rocker angles are the direction when the front wheel moves up relative to its position at the 0° point, and negative rocker angles are the direction when the front wheel moves down relative to its position at the 0° point. The range of motion of each rocker is from [+20°] to [-20°], as shown in Figure 24.

Each of the two bogies is independent, together forming the remaining two degrees of freedom. The middle and rear wheel and the bogie to which they are mounted are fixed with respect to each other and rotate as a unit about their mounting to the rocker as they comply with the surface.

The 0° point corresponds to the angle of the bogie with respect to its rocker when the vehicle sits on a flat horizontal surface. For each bogie, positive bogie angles are the direction when the middle wheel moves up relative to the 0° point and negative bogie angles are when the middle wheel moves down with respect to this point. The range of motion of each bogie is from [+44°] to [-44°], as shown in Figure 24.

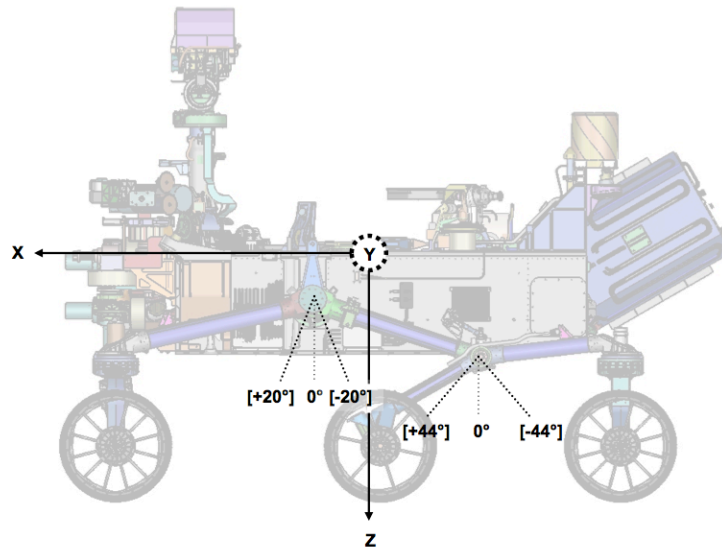


**Figure 24. Suspension sensor 0° references and + and - range of motion (the rover mechanical frame Y vector is into the page)**

### 2.2.2.4 Mobility Forward Kinematics

(Note that flight and ground software may implement different, but mathematically equivalent, representations of mobility kinematics.)

The configuration of the mobility system relative to the rover mechanical frame can be described mathematically by attaching coordinate systems to each of the articulated joints. The origin of each drive wheel frame is defined as the intersection of the steering and driving axes for that wheel. Since rotation of the drive actuators does not change the configuration of the mobility system, we omit them here. We include the middle wheels by treating them as if they had steering actuators with no range of motion.

We follow the standard convention of aligning the Z-axis of each frame with the axis of rotation to which it is attached. For the rockers and bogies, positive Z aligns with positive Y of the rover mechanical frame, and points to the right, consistent with positive pitch upward in front. For the wheels, positive Z aligns with positive Z of the rover mechanical frame when the rover is on a flat surface.

We locate the origins of the rocker and bogie frames along their respective axes at the joint where the next link is attached. We locate the origins of the wheel axes at the center of the wheel (which is along the steering axis for each corner wheel). We include a differential frame to which fiducials described in Section 2.2.2.5 are attached.

Because this is not a single kinematic chain, we cannot follow the convention of pointing the X-axis of each frame at the next link in the chain: instead, we adopt the convention of aligning positive X of each frame with positive X of the rover mechanical frame (in the direction of forward travel), when the rover is on a flat surface.

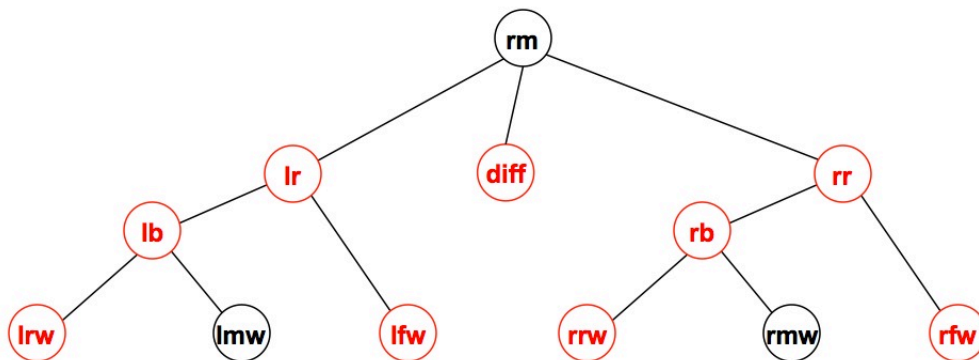
Positive Y completes the right-handed system for each frame.

Table 13 lists the set of mobility frames.

**Table 13. Mobility frame names**

Frame	Designation	Frame Manager Name
rover mechanical	rm	RMECH
differential	diff	(none)
left rocker	lr	ROCKER_L
left bogie	lb	BOGIE_L
left front wheel	lfw	WHEEL_LF
left middle wheel	lmw	WHEEL_LM
left rear wheel	lrw	WHEEL_LR
right rocker	rr	ROCKER_R
right bogie	rb	BOGIE_R
right front wheel	rfr	WHEEL_RF
right middle wheel	rmw	WHEEL_RM
right rear wheel	rrw	WHEEL_RR

The topology of the set of mobility frames is illustrated in Figure 25. Red indicates articulated joints.



**Figure 25. Mobility frame tree**

The orientation of these frames is shown in Figure 26.

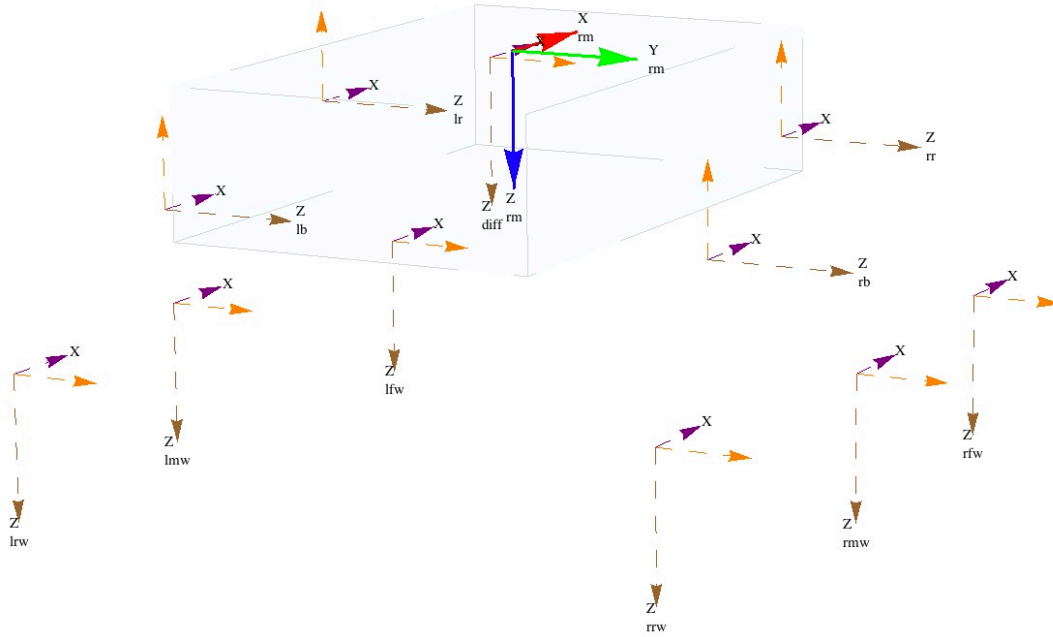


**Figure 26. Mobility suspension and steering frame orientations**

Rotation and translation matrices relating each frame to its predecessor in the kinematic tree are presented in Table 14 and Table 15. Note that the differential and right rocker frames are defined here relative to the left rocker angle.

**Table 14. Rotation matrices relating mobility frames to their parent frames**

Frame	Names	Direction Cosine Matrices		
differential	$RM_{C^{DIFF}}$	$\cos(.2121 \theta_{lr})$	$\sin(.2121 \theta_{lr})$	0
		$-\sin(.2121 \theta_{lr})$	$\cos(.2121 \theta_{lr})$	0
		0	0	1
left rocker	$RM_{C^{LR}}$	$\cos(\theta_{lr})$	$-\sin(\theta_{lr})$	0
		0	0	1
		$-\sin(\theta_{lr})$	$-\cos(\theta_{lr})$	0
left bogie	$LR_{C^{LB}}$	$\cos(\theta_{lb})$	$-\sin(\theta_{lb})$	0
		$\sin(\theta_{lb})$	$\cos(\theta_{lb})$	0
		0	0	1
left front wheel	$LR_{C^{LFW}}$	$\cos(\theta_{lfw})$	$-\sin(\theta_{lfw})$	0
		0	0	-1
		$\sin(\theta_{lfw})$	$\cos(\theta_{lfw})$	0

left middle wheel	$LB_{C^{LMW}}$	1 0 0	0 0 1	0 -1 0
left rear wheel	$LB_{C^{LRW}}$	$\cos(\theta_{lrw})$ 0 $\sin(\theta_{lrw})$	$-\sin(\theta_{lrw})$ 0 $\cos(\theta_{lrw})$	0 -1 0
right rocker	$RM_{C^{RR}}$	$\cos(\theta_{lr})$ 0 $-\sin(\theta_{lr})$	$-\sin(\theta_{lr})$ 0 $-\cos(\theta_{lr})$	0 1 0
right bogie	$RR_{C^{RB}}$	$\cos(\theta_{rb})$ $\sin(\theta_{rb})$ 0	$-\sin(\theta_{rb})$ $\cos(\theta_{rb})$ 0	0 0 1
right front wheel	$RR_{C^{RFW}}$	$\cos(\theta_{rfw})$ 0 $\sin(\theta_{rfw})$	$-\sin(\theta_{rfw})$ 0 $\cos(\theta_{rfw})$	0 -1 0
right middle wheel	$RB_{C^{RMW}}$	1 0 0	0 0 1	0 -1 0
right rear wheel	$RB_{C^{RRW}}$	$\cos(\theta_{rrw})$ 0 $\sin(\theta_{rrw})$	$-\sin(\theta_{rrw})$ 0 $\cos(\theta_{rrw})$	0 -1 0

**Table 15. Translational offsets relating mobility frames to their parent frames**

Joint Frame	Reference Frame	Names	Translation Offset to the Origin of the Joint Frame
differential	RM	$RM_{T^{DIFF}}$	X [-142.00] mm Y [0] mm Z 0 mm in rover mechanical frame
left rocker	RM	$RM_{T^{LR}}$	X [214.00] mm Y -799.59 mm Z [240.50] mm in rover mechanical frame

left bogie	left rocker	$LR_TLB$	X	[-754.00]	mm
			Y	[-230.00]	mm
			Z	-120.00	mm
			in left rocker frame		
left front wheel	left rocker	$LR_TLFW$	X	[881.00]	mm
			Y	[-630.00]	mm
			Z	[-262.91]	mm
			in left rocker frame		
left middle wheel	left bogie	$LB_TLMW$	X	[449.98]	mm
			Y	[-400.00]	mm
			Z	[-264.91]	mm
			in left bogie frame		
left rear wheel	left bogie	$LB_TLRW$	X	[-625.00]	mm
			Y	[-400.00]	mm
			Z	[-142.91]	mm
			in left bogie frame		
right rocker	RM	$RM_TRR$	X	[214.00]	mm
			Y	799.59	mm
			Z	[240.50]	mm
			in rover mechanical frame		
right bogie	right rocker	$RR_TRB$	X	[-754.00]	mm
			Y	[-230.00]	mm
			Z	120.00	mm
			in right rocker frame		
right front wheel	right rocker	$RR_TRFW$	X	[881.00]	mm
			Y	[-630.00]	mm
			Z	[262.91]	mm
			in right rocker frame		
right middle wheel	right bogie	$RB_TRMW$	X	[449.98]	mm
			Y	[-400.00]	mm
			Z	[264.91]	mm
			in right bogie frame		
right rear wheel	right bogie	$RB_TRRW$	X	[-625.00]	mm
			Y	[-400.00]	mm
			Z	[142.91]	mm
			in right bogie frame		

Because the assignment location of the rocker and bogie frames along their axes of rotations makes no kinematic difference, these four measurements are not needed in ATLO.

The location of any frame N with respect to frame L, when rotations and translations relating N to M and M to L are known, is given by

$${}^L T^N = {}^L C^M \cdot M_T^N + {}^L T^M$$

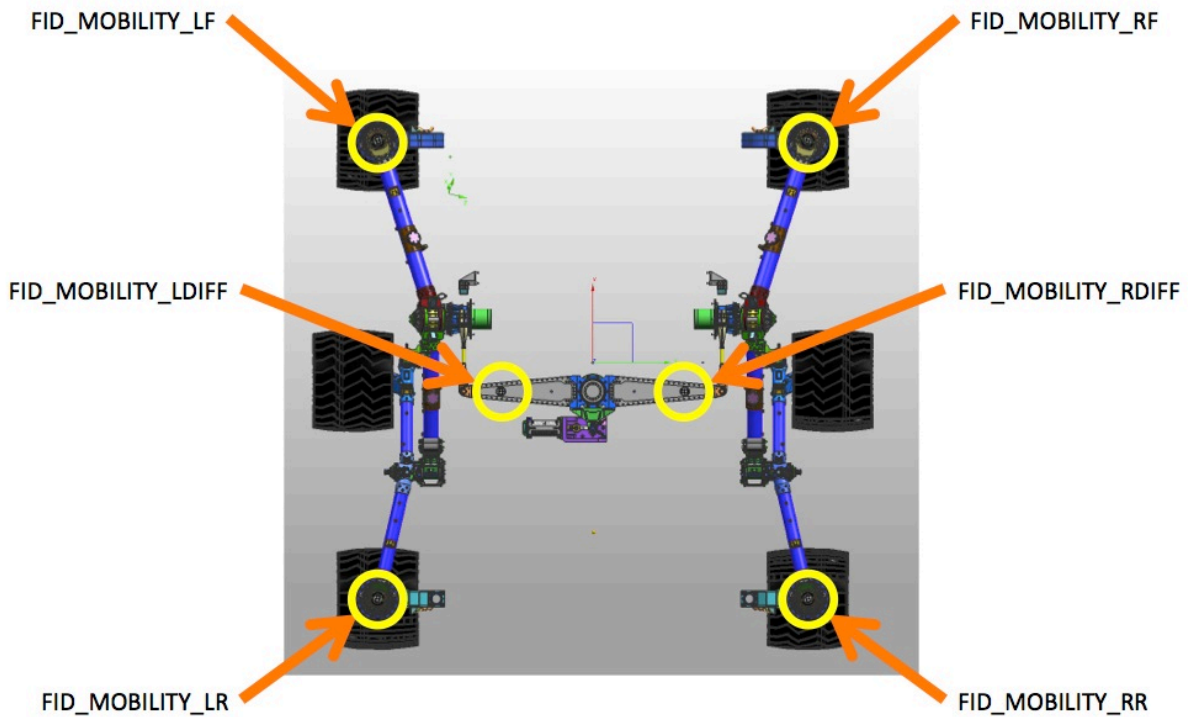
The orientation of any frame N with respect to frame L, when rotations relating N to M and M to L are known, is given by

$${}^L C^N = {}^L C^M \cdot M_C^N$$

Successive application of these relationships can be used to compute the locations and orientations of all eleven mobility frames with respect to the rover mechanical frame.

### 2.2.2.5 Mobility-mounted Fiducials

There are six fiducials mounted to the mobility system, as illustrated in Figure 27 and listed in Table 16.



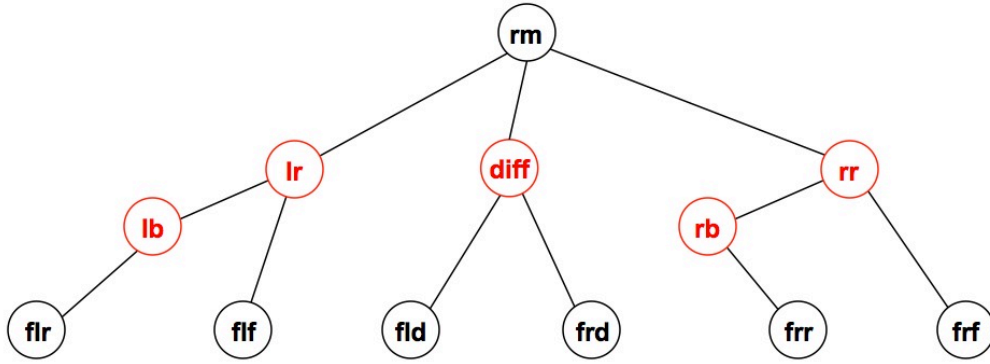
**Figure 27. Fiducials mounted on the mobility system**

Table 16 lists the set fiducials mounted on the mobility system.

**Table 16. Mobility fiducial names**

Fiducial	Designation	Frame Manager Name
fiducial left differential	fld	FID_MOBILITY_LDIFF
fiducial left front	flf	FID_MOBILITY_LF
fiducial left rear	flr	FID_MOBILITY_LR
fiducial right differential	frd	FID_MOBILITY_RDIFF
fiducial right front	frf	FID_MOBILITY_RF
fiducial right rear	fr	FID_MOBILITY_RR

The topology of the set of mobility fiducials is illustrated in Figure 28. Note that the rover mechanical frame and articulated frames are the same as those shown in Figure 25.



**Figure 28. Mobility fiducial frame tree**

Vectors to the centers of mobility fiducials relative to frames in the kinematic tree to which they are attached are presented in Table 17.

**Table 17. Translational offsets relating the centers of mobility fiducials to their parent frames**

Fiducial	Reference Frame	Names	Vector to the Center of the Fiducial
left differential	differential	$DIFF_{T^{FLD}}$	X [0] mm Y [-454.43] mm Z [-53.51] mm in differential frame
left front	left rocker	$LR_{T^{FLF}}$	X [881.00] mm Y [-37.50] mm Z [-262.91] mm in left rocker frame
left rear	left bogie	$LB_{T^{FLR}}$	X [-625.00] mm Y [193.00] mm Z [-142.91] mm in left bogie frame
right differential	differential	$DIFF_{T^{FRD}}$	X [0] mm Y [454.43] mm Z [-53.51] mm in differential frame
right front	right rocker	$RR_{T^{FRF}}$	X [881.00] mm Y [-37.50] mm Z [262.91] mm in right rocker frame
right rear	right bogie	$RB_{T^{FRR}}$	X [-625.00] mm Y [193.00] mm Z [142.91] mm in right bogie frame